Available online at www.sciencedirect.com
SCIENCE DIRECT®
Physica E 34 (2006) 662–665
PHYSICA E
www.elsevier.com/locate/physe

Charge pumping in carbon nanotubes

V.I. Talyanskii[a,*], P. Leek[a], M. Buitelaar[a], C.G. Smith[a], D. Anderson[a], G. Jones[a], J. Wei[b], D. Cobden[b]

[a]Cavendish Laboratory, University of Cambridge, Madingley Road, Cambridge, CB3 0HE, UK
[b]Department of Physics, University of Washington, Seattle, WA

Available online 18 April 2006

Abstract

We demonstrate charge pumping in semiconducting carbon nanotubes by a traveling potential wave. From the observation of pumping in the nanotube insulating state we deduce that transport occurs by packets of charge being carried along by the wave. By tuning the potential of a side gate, transport of either electron or hole packets can be realized. Prospects for realization of nanotube-based single electron pumps are discussed.

PACS: 73.23.Hk; 73.63.Fg; 85.35.Kt

Keywords: Nanotubes; Nanotube devices; Coulomb blockade

The phenomenon of charge pumping has attracted considerable interest in the last two decades [1–12]. In pumping, a periodic in time and spatially nonhomogeneous external perturbation yields a DC current. If a fixed number (n) of electrons is transferred during a cycle, then the current is quantized in the units of ef, where e is the electron charge and f is the perturbation frequency.

Previously quantized current $I = nef$ has been observed in two different ways: first, using devices comprising charge islands and controlled by a number of phase-shifted AC signals [3,4,8], and second, using one-dimensional (1D) channels within a GaAs heterojunction where a surface acoustic wave (SAW) produces traveling potential wells which convey packets of electrons along the channel [5]. In the SAW pumps, transport of charge resembles the pumping of water by an Archimedean screw [7], and when this principle is combined with Coulomb blockade, it results in pumping a fixed number of electrons n per cycle [5].

The carbon nanotubes (CNs) have significant advantages over semiconductor and metallic systems in terms of single electron pumping [9,10]. The typical Coulomb charging energies achievable in CNs can be reaching 10 meV, significantly larger than in the pumps described in Refs. [3–5,8]. CNs also offer advantages in the quantum regime of pumping [1] due to an order of magnitude larger minigaps achievable [9]. However, experimentally the charge pumping in CNs has not been studied.

In this work we demonstrate realization of electron pumping in a semiconducting CN, present its essential experimental characteristics, and discuss possible applications of the discovered effects.

Fig. 1a shows the schematic of the experiment. We used a traveling potential wave of a SAW as an external pumping perturbation. A CN (grown by chemical vapour deposition [13]) lies on a polished 36° Y-cut quartz substrate. Source and drain contacts (separated by 1 μm), a side gate, and a transducer for SAW generation are fabricated by electron beam lithography.

The transducer generates a SAW with a wavelength of 1 μm corresponding to a SAW frequency of 3.2 GHz. Since quartz is piezoelectric, SAW is accompanied by an electrostatic potential wave which acts on the electrons in the CN. All the data presented here are for a CN of diameter 2.5 ± 0.5 nm at $T = 5$ K.

Fig. 2a presents the current as a function of source-drain bias (V_{sd}) and gate voltage (V_g) in the absence of a SAW

*Corresponding author. Tel./fax: +44 1223 337 388.
E-mail address: vit10@cam.ac.uk (V.I. Talyanskii).

1386-9477/$ - see front matter
doi:10.1016/j.physe.2006.03.054

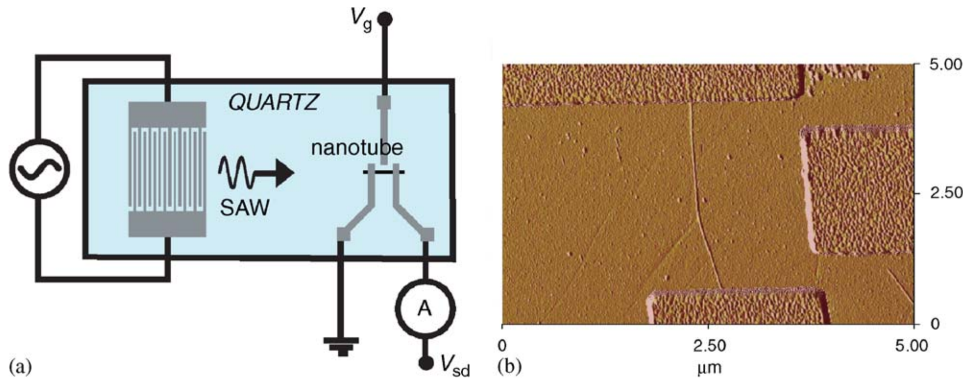

Fig. 1. (a) Schematic of the device. The transducer on the left generates a SAW. (b) AFM image of the contacted CN.

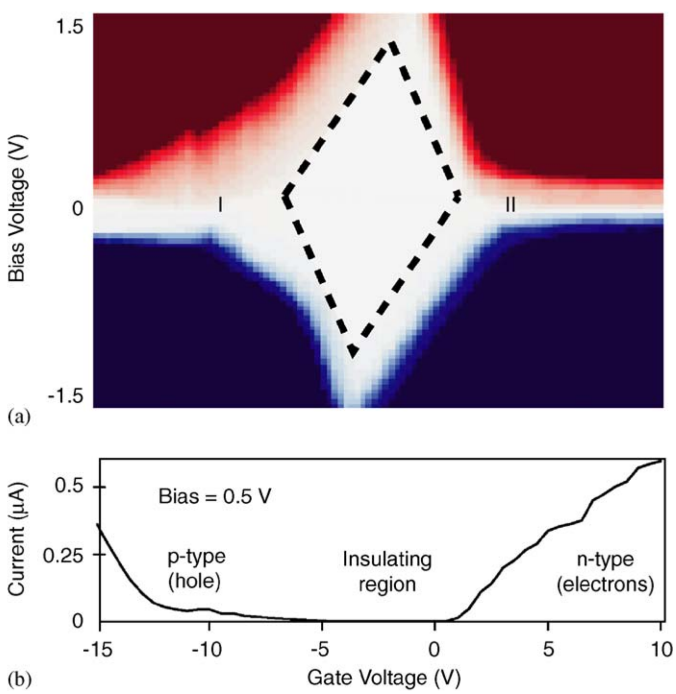

Fig. 2. (a) Colourscale plot of the DC current versus V_g and V_{sd} at a temperature of 5 K. Red indicates positive and blue negative currents. The superimposed rhomboid indicates the location of the insulating region, centred on $V_g = -2.5\,V$. (b) Line scan taken from the colourscale plot, at $V_{sd} = 0.5\,V$.

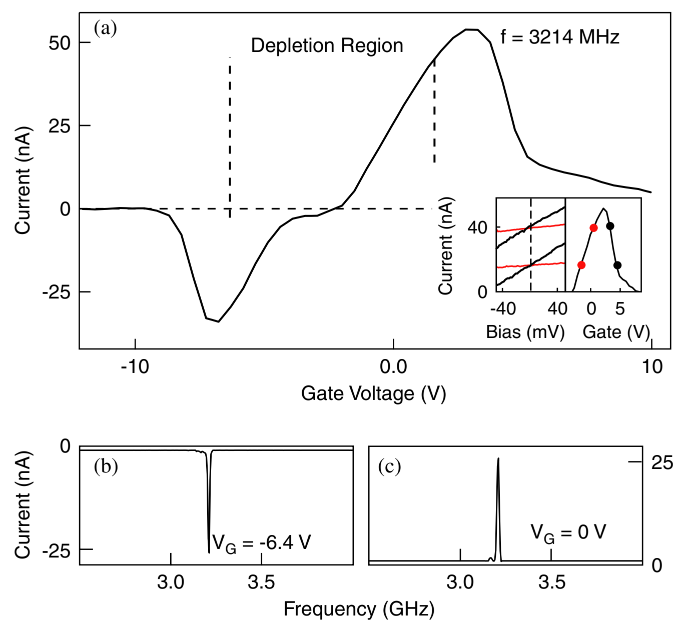

Fig. 3. (a) Dependence of the SAW-induced current on gate voltage. (Inset) dependence of the current on DC bias for four fixed values of the gate voltage. (b,c) Dependence of the SAW-induced current on RF frequency for two values of the gate voltage.

excitation. The data in Fig. 2 shows that this CN is semiconducting.

Applying RF power P_{RF} to the transducer induces a DC current I_{SAW} in the CN at $V_{sd} = 0$. The current is generated only within a narrow frequency range corresponding to the passband of the transducer (Figs. 3b and c). Fig. 3a shows the variation of I_{SAW} with V_g at $P_{RF} = 20\,dB\,m$ (100 mW). At this power, the current is present across the entire gate region in which the low-bias DC conductance is absent, reversing direction in the centre and showing a peak located just outside the insulating region in each direction. At lower power levels there is a range of V_g in which I_{SAW} is zero (Fig. 4), and as the power level decreases this range widens.

For interpretation of the results in Figs. 2–4, it is convenient to start by noticing that the pumping current flows in the insulating state of the CN ($-5\,V < V_g < 1\,V$) where there are no free carriers in the bulk of the CN in the absence of the SAW. It implies that SAW must inject the carriers into the CN from the source contact. When injected, the carriers become trapped in SAW potential minima (or maxima for holes), and carried along the CN by the wave. Thus, the observation of a SAW-induced current in the insulating state of the CN leads us to a model of transport in the form of charge packets moving with SAW.

The transport in the packets is illustrated in Fig. 5. The panels show the electrons and holes injection, for the gate voltage at which the Fermi level is in the centre of the semiconducting gap ($V_g \sim -2.5\,V$).

In Fig. 5 we neglect the relatively small difference in barrier height for the electrons and holes at the contacts.

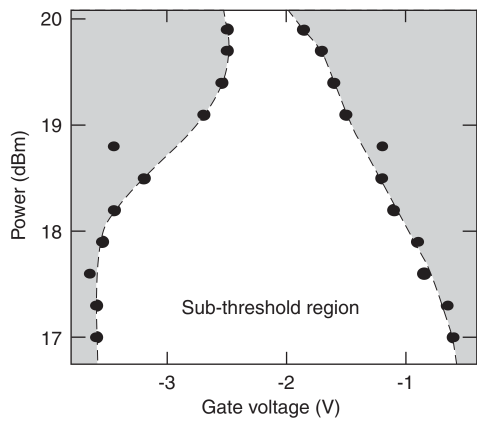

Fig. 4. Points correspond to $|I_{SAW}| = 0.1$ nA. This small threshold current was arbitrarily chosen to indicate the region in the P–V_g plane in which a SAW-induced current is absent. The dashed lines are guides to the eye.

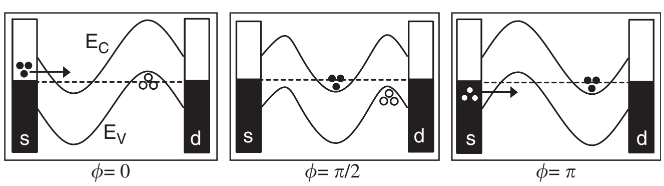

Fig. 5. Schematic band diagrams depicting the proposed mechanism of charge transport by the SAW at a gate voltage where the CN is otherwise insulating.

We also assume that the injection takes place when the SAW electric field is at its maximum at the source contact. The SAW bends the conduction and valence bands of the CN so that when the bottom (top) of the conduction (valence) band is below (above) the Fermi level of the source contact, electrons (holes) can tunnel into the CN. Thus, the SAW amplitude must exceed a threshold value for the injection of charge to be possible. With the Fermi level in the centre of the gap, the thresholds for electron and hole injection are the same, and the threshold SAW field is related to the semiconducting gap: $E_{gap} = 2e\Phi_{SAW} \sim 0.4$ V, at $P_{RF} = +20$ dB m applied to the transducer (from the geometry of the transducer we estimated $\Phi_{SAW} \sim 0.2$ V at $P_{RF} = +20$ dB m). This amplitude only slightly exceeds the threshold, resulting in an estimate $E_{gap} \sim 0.4$ eV, in reasonable agreement with the theoretical value 0.3 eV for semiconducting CNs of diameter ~2.5 nm [14].

For SAW amplitudes exceeding the threshold value ($\Phi_{SAW} \geqslant E_{gap}/2e$), the current crosses zero at some particular gate voltage ($V_g \sim -2.5$ V in Fig. 3). At this value of V_g the electron and hole packets contain the same number of particles, resulting in zero net current. If V_g is made more positive from this point, the electron packets become bigger than the hole packets so there is a net positive current. Above some V_g the threshold condition for hole injection is not met and the current is carried entirely by electron packets. Likewise, as V_g is made more negative, the hole packets become bigger and the net current is negative, and beyond some point it is carried only by holes.

When the SAW amplitude is below the threshold value ($\Phi_{SAW} < E_{gap}/2e$), a threshold for the injection of either electrons or holes (Fig. 4) can be reached by adjusting the position of the bands with respect to the Fermi level (using V_g), but simultaneous transport of both electron and hole packets should not be possible at any V_g.

Exceeding the threshold is a necessary but not sufficient condition for effective charge injection. A strong enough electric field must also be present at the source contact to make the tunneling barriers transparent for electrons and holes. As the same condition determines the DC bias V_{sd} required to drive a DC current (Fig. 2) we can compare the SAW electric field to that occurring in this case. In our device a DC current is switched on at a bias of 1.5 V, (Fig. 2a) giving an average electric field of ~1.5 V/μm along the CN. The maximum electric field due to the SAW at $P_{RF} = +20$ dB m is indeed close to this value at $E_{max} = 2\pi\Phi_{SAW}/\lambda \sim 1.3$ V/μm. Thus the comparison of the DC and SAW threshold fields corroborates our model of the transport in packets. We note that the actual electric field (caused either by DC bias or by the SAW) can be significantly enhanced in a region very close to a thin contact strip due to geometrical factors.

We have until now limited our discussion of the SAW-induced current to the range of V_g in which the DC conductance is zero. Outside this range the current shows distinct peaks, after which it drops dramatically (Fig. 3a). We suggest that outside the insulating region the free carriers screen the SAW field and the carriers are delocalized, so that the description of transport in charge packets does not apply. In the "drag" regime the DC current is proportional to the momentum transfer from the wave to the electronic system [15]. In this picture, the peaks in current in Fig. 3a manifest a crossover from the transport in packets to the drag-type transport regime. This assertion about the change of the transport mechanism can be tested since the charge packet transport should be little affected by a DC bias, whereas outside the insulating region where free carriers exist in the CN, the effect of a bias is expected to be much stronger. Such behaviour is indeed observed (inset of Fig. 3a).

We conclude with a discussion on the feasibility of pumping single electrons in carbon CNs. The classical mechanism of SAW single electron pumping should be observable for the semiconducting CNs studied here. In that mechanism the number of electrons in the packet is fixed due to Coulomb interactions. This work shows that the transport of charge in the form of packets, which can be thought of as moving quantum dots, can be realized. For single-electron pumping each dot should be populated with the same number of electrons, and the conditions at the source contact where the SAW "quantum dot" is filled with electrons (holes) become crucial. The conditions at the source contact can be improved by using a better (less resistive) source contact, such as Pd. A more radical solution would be to induce electrons or holes in a section of a CN adjacent to the source electrode with the help of an additional side gate. Then, as with the GaAs SAW pumps [5], the filling of a SAW potential well with carriers will not involve a slow tunneling process and the quantized transport regime should be observable.

This work was supported by the EPSRC UK (grant GR/R67521) and the EC program SAWPHOTON. VT and PL acknowledge support from the Newton Trust and the National Physical Laboratory, respectively.

References

[1] D.J. Thouless, Phys. Rev. B 27 (1983) 6083.
[2] Q. Niu, D.J. Thouless, J. Phys. A 17 (1984) 2453.
[3] L.J. Geerligs, et al., Phys. Rev. Lett. 64 (1990) 2691.
[4] L.P. Kouwenhoven, et al., Phys. Rev. Lett. 67 (1991) 1626.
[5] V.I. Talyanskii, et al., Phys. Rev. B 56 (1997) 15180.
[6] M. Switkes, et al., Science 283 (1999) 1905.
[7] B.L. Altshuler, L.I. Glazman, Science 283 (1999) 1864.
[8] M.W. Keller, et al., Science 285 (1999) 1706.
[9] V.I. Talyanskii, et al., Phys. Rev. Lett. 87 (2001) 276802.
[10] P. Sharma, C. Chamon, Phys. Rev. Lett. 87 (2001) 96401.
[11] D.S. Novikov, cond-mat/0412456, 2005.
[12] J. Ebbecke, et al., Phys. Rev. B 70 (2004) 233401.
[13] J. Kong, et al., Chem. Phys. Lett. 292 (1998) 567.
[14] R. Saito, G. Dresselhaus, M.S. Dresselhaus, in: Physical Properties of Carbon Nanotubes, Imperial College Press, London, 1999, pp. 66–70.
[15] A. Wixforth, et al., Phys. Rev. Lett. 56 (1986) 2104.